J|A|C|S
ARTICLES
Published on Web 12/09/2003

Intramolecular Cycloadditions of Cyclobutadiene with Dienes: Experimental and Computational Studies of the Competing (2 + 2) and (4 + 2) Modes of Reaction

John Limanto,[†,‡] Kelli S. Khuong,[§] K. N. Houk,*[,§] and Marc L. Snapper*[,†]

Contribution from the Department of Chemistry, Merkert Chemistry Center, Boston College, 2609 Beacon Street, Chestnut Hill, Massachusetts 02467, and the Department of Chemistry and Biochemistry, University of California, Los Angeles, California 90095-1569

Received August 21, 2003; E-mail: houk@chem.ucla.edu; marc.snapper@BC.edu

Abstract: Highly functionalized, cyclobutene-containing adducts are afforded through intramolecular cycloadditions between cyclobutadiene and tethered dienes. The cycloaddition displays the following reactivity trend: cyclobutadiene serves as a dienophile in intramolecular reactions when it is connected to the diene through a four-atom tether. In cases where a three-atom linker separates the two reaction partners, the cyclobutadiene can function as both a diene and dienophile, affording a mixture of vinylcyclobutane (2 + 2) and cyclohexene-containing cycloadducts (4 + 2). Theoretical studies provide insight into the factors influencing the various pericyclic pathways operative in this system. In cases where cyclobutadiene functions as a diene to generate vinylcyclobutanes, these (2 + 2) adducts can be converted into the corresponding (4 + 2) cyclohexenyl products through a [3,3]-sigmatropic rearrangement.

Introduction

Cyclobutadiene (**2**) is a reactive, antiaromatic species[1] that can be generated through oxidation of its corresponding iron tricarbonyl complex **1**. Cyclobutadiene undergoes rapid dimerization,[2] or when generated in the presence of π-systems such as olefins or dienes,[3] it undergoes intermolecular Diels−Alder (DA) reactions that lead to a variety of cyclobutene-containing adducts (eqs 1 and 2). Cyclobutadiene can serve as either a diene or dienophile in these [4 + 2] cycloadditions.

intermolecular cycloadditions

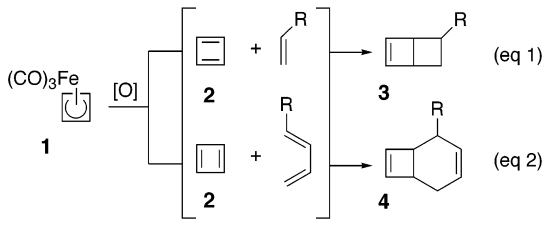

We envisioned that an *intramolecular* DA reaction between cyclobutadiene and dienes could offer unique opportunities for generating novel cyclobutene-containing cycloadducts. Of particular interest is that two modes of cycloaddition are plausible. In one mode, cyclobutadiene serves as a diene providing fused cyclobutane-containing products **6** (eq 3). Such a reaction can be described formally as a [4 + 2] cycloaddition (Woodward−Hoffmann notation, using brackets, where the numbers refer to the electrons involved in bonding changes)[4] or, alternatively, as a (2 + 2) cycloaddition (Huisgen notation, using parentheses, where the numbers refer to the atoms involved in the forming ring).[5] In a second mode of reactivity, cyclobutadiene serves as a dienophile to generate cyclohexene-containing products **7** (eq 4). This reaction is also a [4 + 2] cycloaddition according to Woodward−Hoffmann notation and is now a (4 + 2) cycloaddition according to the Huisgen notation. Because the Huisgen notation differentiates between these two pathways, (2 + 2) and (4 + 2) notation will be used throughout the remainder of the text. It should be noted, however, that both reactions are symmetry-allowed [4 + 2] cycloadditions. On the basis of earlier intermolecular transformations, we anticipated that the (4 + 2) cycloaddition (eq 4) should predominate over the (2 + 2) process;[6] however, the influence of the tether on this intramolecular variant was unclear.

Our preliminary studies have demonstrated the feasibility of intramolecular DA reactions of cyclobutadiene with dienes and olefins.[7] These investigations have led to efficient new methods for the preparation of a variety of cyclobutene-containing

[†] Boston College.
[‡] Current address: Merck & Co., Inc., RY800-C264, P.O. Box 2000, Rahway, NJ 07065.
[§] University of California, Los Angeles.

(1) (a) Maier, G. *Angew. Chem., Int. Ed. Engl.* **1974**, *13*, 425. (b) Deniz, A. A.; Peters, K. S.; Snyder, G. J. *Science* **1999**, *286*, 1119.
(2) Li, Y.; Houk, K. N. *J. Am. Chem. Soc.* **1996**, *118*, 880 and references therein.
(3) Watt, L.; Fitzpatrick, J. D.; Pettit, R. *J. Am. Chem. Soc.* **1966**, *88*, 623.
(4) Woodward, R. B.; Hoffmann, R. *Angew. Chem., Int. Ed. Engl.* **1969**, *8*, 781.
(5) (a) Huisgen, R. *Angew. Chem., Int. Ed. Engl.* **1968**, *7*, 321. (b) Huisgen, R.; Grashey, R.; Sauer, J. In *The Chemistry of Alkenes*; Patai, S., Ed.; Wiley Interscience: London, 1964; p 739.
(6) Barborak, J. C.; Pettit, R. *J. Am. Chem. Soc.* **1967**, *89*, 3080.
(7) For an initial report on intramolecular cyclobutadiene cycloadditions with dienes, see: (a) Limanto, J.; Snapper, M. L. *J. Org. Chem.* **1998**, *63*, 6440. For intramolecular cycloadditions with olefins, see: (b) Tallarico, J. A.; Randall, M. L.; Snapper, M. L. *J. Am. Chem. Soc.* **1996**, *118*, 9196. (c) Limanto, J.; Tallarico, J. A.; Porter, J. R.; Khuong, K. S.; Houk, K. N.; Snapper, M. L. *J. Am. Chem. Soc.* **2002**, 124, 14748.

10.1021/ja0380547 CCC: $25.00

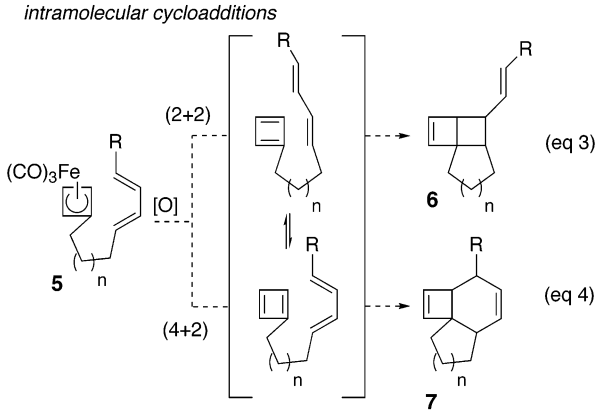

adducts that have then been used to access medium-sized ring-containing compounds of interest.[8] In general, the success of the cycloaddition was found to be dependent on the nature of the tether connecting the two reactive cycloaddition partners. In this regard, we report herein our experimental and theoretical findings on the features that influence the intramolecular cycloadditions of cyclobutadiene with dienes.

Previous studies indicate that an efficient intramolecular (2 + 2) cycloaddition between cyclobutadiene and olefins can proceed if they possess an activation barrier ($\Delta G^{\ddagger}$) of less than ~13.5 kcal/mol.[7c] When the barrier exceeds 13.5 kcal/mol, the facile intermolecular dimerization of cyclobutadiene becomes competitive, and yields of the intramolecular cycloadducts drop. The barrier and, therefore, the ease of the intramolecular DA were found to be highly dependent on the nature of both the tether and the alkene. The three-atom ethereal tether appeared to be ideal for the optimal intramolecular (2 + 2) cycloaddition geometry. Activation of the alkene by an electron-withdrawing group also proved a successful strategy leading to lower activation energies and increased yields of desired cycloadducts.

In conjunction with experimental studies, theoretical density functional calculations (B3LYP/6-31G*) have been extended to the study of intramolecular cycloadditions between cyclobutadiene and dienes. The goals of the computational study are to understand (1) the intermolecular reactivity of cyclobutadienes with butadiene, (2) the influence of the tether on the intramolecular reactivity, and (3) the inter- and intramolecular reactivity of cyclic dienes with cyclobutadiene.

Results and Discussion

The influence of tether length and tether substituents as well as the stereochemistry and electronic properties of the diene in the intramolecular cycloadditions with cyclobutadiene are described. Along with structural and electronic factors, the manner in which the cyclobutadiene is generated is also shown to affect the efficiency of the intramolecular process.

Generation of Cyclobutadiene. The major competing reaction in the intramolecular cycloadditions is the intermolecular dimerization of cyclobutadiene. For substrates well-posed toward the intramolecular reaction, a cerium ammonium nitrate (CAN) oxidation of the iron complex rapidly provides the desired cycloadducts (5 equiv, acetone, 1−2 mM, RT, 15 min). For substrates that lead to a significant amount of cyclobutadiene dimerization under the CAN oxidation conditions, a slower trimethylamine-*N*-oxide (TMAO) oxidation usually provides better yields of the desired cycloadducts (8−20 equiv, acetone, 2−20 mM, reflux, 6−24 h). Overall, the reaction conditions that mimimize the concentration of free cyclobutadiene generally lead to higher yields of the desired intramolecular cycloadducts.

Table 1. Intramolecular Cycloadditions between Cyclobutadiene and Dienes Connected with a Three-Atom, Ether-Containing Linkage

entry	substrate	cycloadducts	yield%;[a] (ratio)
(1)	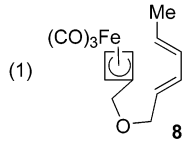	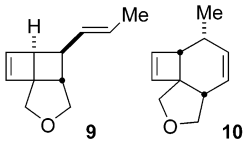 **8** **9** **10**	75% (2.6:1.0)
(2)	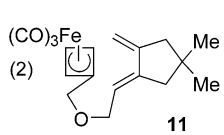	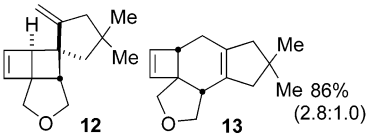 **11** **12** **13**	86% (2.8:1.0)
(3)	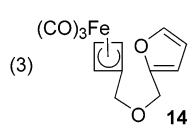	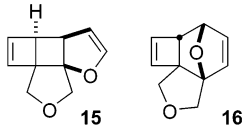 **14** **15** **16**	45% (1.0:3.5)
(4)	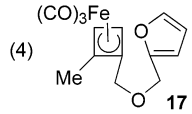	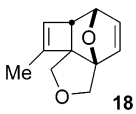 **17** **18**	66%
(5)	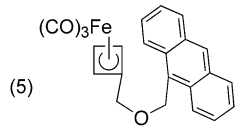	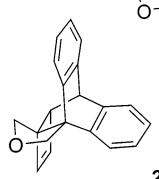 **19** **20**	61%

[a] Reaction conditions: CAN (5 equiv), acetone (1 mM), RT; isolated yield.

Ether-Containing Tethers. Our initial investigation concentrated on tricarbonylcyclobutadiene iron complexes connected to dienes through an ether-containing three-atom linkage (Table 1). As illustrated in entry 1, treatment of substrate **8** with CAN in acetone (1 mM) afforded compound **9** preferentially, as well as some of the (4 + 2) cycloadduct **10** (**9**/**10**, 2.6:1.0) in a combined yield of 75%. One possible explanation for the favoring of (2 + 2) products over (4 + 2) might be that the s-trans conformation of the acyclic diene and the corresponding TS lack the H1−H4 repulsion present in the s-cis conformation and TS. This destabilizing repulsion would be absent from the transition states involving cyclic dienes. Substrate **11**, with a conformationally locked diene that should favor the (4 + 2) mode of cycloaddition, was prepared to investigate this possibility. In a fashion similar to the previous example, oxidative cyclization of complex **11** afforded predominately the (2 + 2) cycloadduct **12**, along with some (4 + 2) product **13** (**12**/**13**, 2.8:1; entry 2). Evidently, the three-atom ethereal linkage allows the (2 + 2) cycloaddition to be competitive with the (4 + 2) pathway, even in a case with a diene locked in the s-cis conformation and possessing a hindered trisubstituted olefin (e.g., entry 2).

(8) (a) Snapper, M. L.; Tallarico, J. A.; Randall, M. L. *J. Am. Chem. Soc.* **1997**, *119*, 1478. (b) Randall, M. L.; Lo, P.; Bonitatebus, P. J., Jr.; Snapper, M. L. *J. Am. Chem. Soc.* **1999**, *121*, 4534. (c) Limanto, J.; Snapper, M. L. *J. Am. Chem. Soc.* **2000**, *122*, 8071. (d) Deak, H. L.; Stokes, S. S.; Snapper, M. L. *J. Am. Chem. Soc.* **2001**, *123*, 5152. (e) Lo, P. C.-K.; Snapper, M. L. *Org. Lett.* **2001**, *3*, 2819.

Table 2. Rearrangement of the (2 + 2) Cycloadducts to the (4 + 2) Products

entry	(2+2) adduct	(4+2) adduct	yield%[a]
(1)	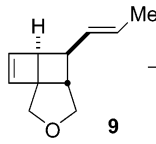	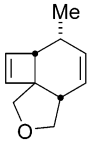	86%
(2)	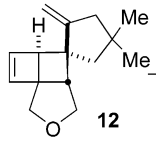	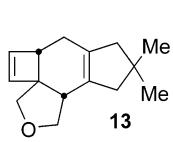	90%
(3)	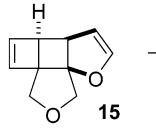	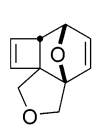	89%

[a] Isomerization conditions: 130 °C, pentanes; isolated yields.

Scheme 1. Origin of the (4 + 2) Cycloadduct

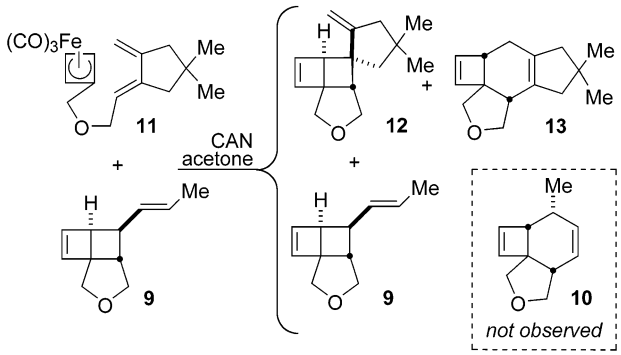

We were interested whether the observed (2 + 2)/(4 + 2) ratio in the reactions reflected the relative rates of two independent cycloadditions or whether the (4 + 2) cycloadduct was generated indirectly from the (2 + 2) product through a [1,3]- or [3,3]-rearrangement. In this regard, we knew that heating the (2 + 2) product **9** converted it entirely to the more stable (4 + 2) cycloadduct **10** (entry 1, Table 2).[9] Insight into the origin of the (4 + 2) product was established by resubjecting the (2 + 2) product to the oxidative cycloaddition conditions (Scheme 1). Complex **11** was oxidized with CAN in the presence of cycloadduct **9**, affording cycloadducts **12** and **13**, as well as returning cycloadduct **9** with no trace of the (4 + 2) product **10**. This observation suggested that the product ratio observed in the oxidative cycloaddition reflects the kinetic selectivity of the two concurrent and independent cycloadditions and rules out the possibility of a room temperature, cerium-catalyzed rearrangement of the (2 + 2) cycloadduct to the (4 + 2) product. NMR analysis (nOe) of the resulting (4 + 2) products indicated that they are the result of an endo cycloaddition process.

While dienes **8** and **11** provided mainly (2 + 2) cycloadducts, aromatic dienes favored the (4 + 2) cycloaddition pathway. As shown in entry 3 of Table 1, treatment of furanyl substrate **14** with CAN afforded cycloadducts **15** and **16** in 45% yield, where the (4 + 2) adduct **16** is now the major product (**15**/**16**, 1.0:3.5). Evidently, the furanyl functionality, while leading to a less efficient cycloaddition overall, favored the (4 + 2) cycloaddition process relative to the (2 + 2) pathway.

Scheme 2. Cycloaddition Possibilities for Complex 17

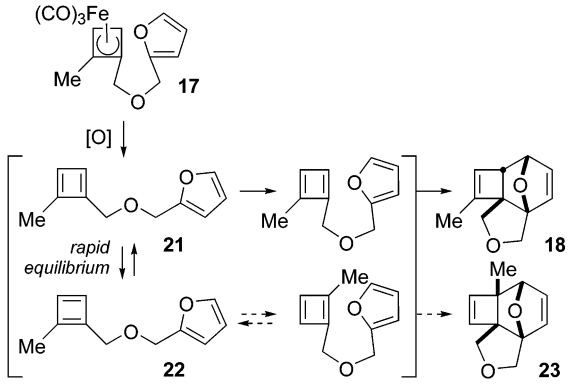

In a similar fashion, oxidation of furanyl substrate **17** leads to the (4 + 2) product **18** as the only identifiable monomeric product. In this case, the ortho-disubstituted cyclobutadiene generated through the oxidative removal of the iron complex can interact in several ways with the furan moiety (Scheme 2). One factor that may be controlling the regiochemistry of the cycloaddition is the preferred tautomer of cyclobutadiene; however, the isomerization between isomers **21** and **22** is expected to be rapid.[10] More likely it is the additional steric interactions of the methyl group in the transition state that disfavor the formation of **23** relative to cycloadduct **18**.

The synthetic utility of these cycloadditions is bolstered by the observation that the (2 + 2) cycloadduct (or the (2 + 2)/(4 + 2) mixture) can be converted thermally to the (4 + 2) product. As described for the rearrangement of cycloadduct **9**, the (2 + 2) products **12** and **15** can be heated in pentane to provide the corresponding (4 + 2) products in 89−90% yields (entries 2 and 3, Table 2). While the nature of the rearrangement was unclear, the reaction sequence offered the cyclohexenyl products in synthetically useful yields. We expected that the rearrangement was occurring through either a [1,3]- or [3,3]-sigmatropic process.

To ascertain the mechanistic course of the rearrangement, the disubstituted iron tricarbonyl complex **24** was prepared and subjected to CAN-promoted cycloaddition conditions (Scheme 3). All four cycloadducts, consisting of two pairs of regioisomers from each mode of cycloaddition, were obtained in 70% overall yield (**25**/**26**/**27**/**28**, 56:20:7:17). The individual (2 + 2) cycloadducts **25** and **26**, upon heating in pentane (130 °C, 3−4 h), afforded only the corresponding (4 + 2) cycloadducts **27** and **28** in 83% and 87% yield, respectively. These results suggest that the regio- and stereospecific thermal isomerization of the (2 + 2) cycloadducts to the (4 + 2) products proceeds through a [3,3]-sigmatropic pathway.

Longer Ether-Containing Tethers. Whereas substrates with an ether-containing three-atom tether generally favor the (2 + 2) mode of cycloaddition (with the exception of the aromatic substrates), the one-carbon homologation of the tether (i.e., four-atom tether) resulted in greater amounts of the (4 + 2) cycloadducts. As shown in Table 3, substrate **29** afforded

(9) AM1 calculations indicated that the (4 + 2) adduct **10** is 16 kcal/mol more stable than the corresponding (2 + 2) cycloadduct **9**.

(10) (a) Carpenter, B. K. *J. Am. Chem. Soc.* **1983**, *105*, 1700. (b) Reeves, P. C.; Devon, T.; Pettit, R. *J. Am. Chem. Soc.* **1969**, *91*, 5890. (c) Reeves, P. C.; Henery, J.; Pettit, R. *J. Am. Chem. Soc.* **1969**, *91*, 5888.

Scheme 3. Mechanistic Course of the Thermal Rearrangement

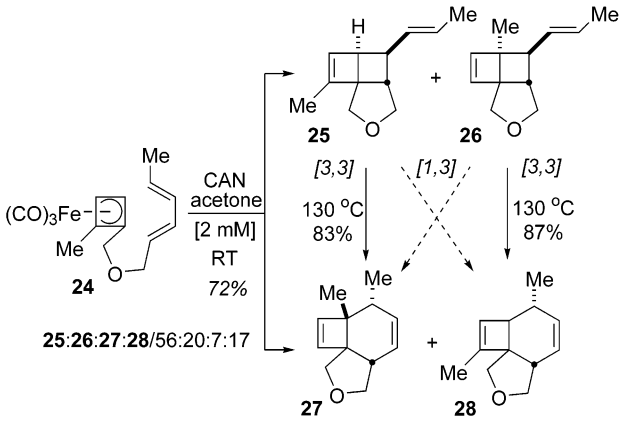

Table 3. Intramolecular Cycloadditions between Cyclobutadiene and Dienes Connected with Ether Linkages

entry	substrate	cycloadducts	methods[a] yield%;[b] (ratio)
(1)	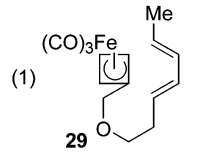	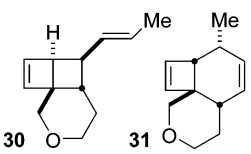	A 75% (1:13)
(2)	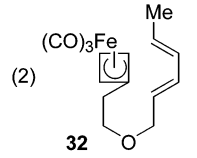	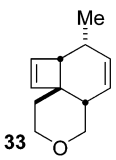	A 60%
(3)	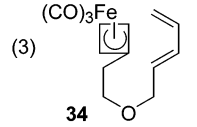	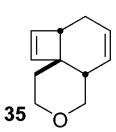	A 66%
(4)	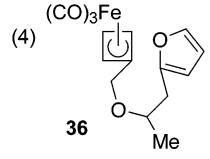	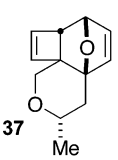	A 41%
(5)	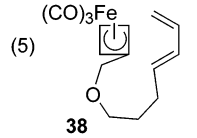	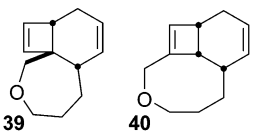	B 28% (2.5:1.0)
(6)	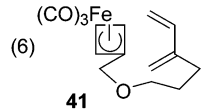	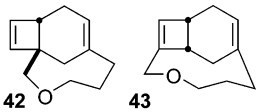	C 32% (**43** only)
(7)	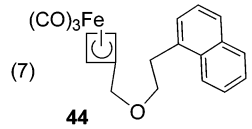	no intramolecular cycloadducts observed	

[a] Reaction conditions. Method A: CAN (5 equiv), acetone (1 mM), RT. Method B: TMAO (20 equiv), acetone (1 mM), reflux. Method C: CAN (10 equiv), MeOH (1 mM), reflux. [b] Isolated yields.

predominantly the (4 + 2) cycloadduct **31** (**31**/**30**, 13:1) in 75% yield. Similarly, the isomeric ethereal complexes **32** and **34** generated only (4 + 2) adducts, **33** and **35** in 60−66% yields,

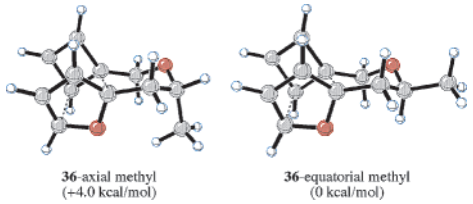

Figure 1. Calculated transition structures for cycloaddition of **36** with axial and equatorial methyl group leading to cycloadduct **37** and the unobserved diastereomer.

Scheme 4. Preference for endo Conformation in Cycloaddition Transition State May Control Product Distribution

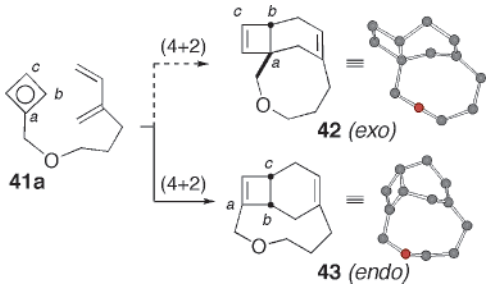

respectively. It is uncertain in these examples whether the absence of (2 + 2) cycloadducts represents the inherent reactivity of the system or our inability to locate the minor (2 + 2) isomers. In either case, the (4 + 2) pathway is favored. While it is clear that an increase in tether length is detrimental to the (2 + 2) cycloaddition,[7c] these results suggest that the (4 + 2) pathway is less sensitive to that trend. Interestingly, the longer tether appears to offer greater levels of diastereoselectivity in the (4 + 2) cycloadditions; the four-atom tether aromatic substrate **36** provided the (4 + 2) cycloadduct **37** as a single diastereostereomer (entry 4, Table 3). In this case, the selectivity appears to arise by avoiding 1,3-interactions in the transition state by placing the methyl group in an equatorial position on the nascent six-membered ring (Figure 1).

In line with the above-mentioned observations, when an even longer tether is used in the reaction, only the (4 + 2) cycloaddition is operative, albeit with reduced efficiency. While no intramolecular cycloadducts were obtained under the rapid CAN oxidation conditions for the five-atom tether complex **38**, subjection of this substrate to the slower oxidant, TMAO in refluxing acetone, afforded the two regiomeric (4 + 2) products **39** and **40** (**39**/**40**, 2.5:1) in a 28% combined yield (entry 5, Table 3). In comparison, subjection of the type II Diels−Alder substrate **41** to modified CAN reaction conditions (10 equiv, refluxing MeOH, 3 min) produced cycloadduct **43** in 32% yield (but not **42**), as well as byproducts resulting from cyclobutadiene dimerizations (entry 6). The formation of adduct **43** is likely due to the preference for an endo conformation in the cycloaddition transition state; a conformation not readily accessible for the formation of compound **42** (Scheme 4).

All-Carbon Linkage. As illustrated in Table 4, treatment of the all-carbon three-atom tether-containing alcohol **45** with CAN afforded both the (2 + 2) adduct **46** and the (4 + 2) adduct **47** (**46**/**47**, 1:1.8), *each as a single diastereomer* in 70% overall yield (entry 1). This result illustrates the delicate balance and subtle nuances between the various cycloaddition pathways. In this case, the energy differences in the transition states leading to diastereomers for *either* the (2 + 2) or the (4 + 2) cycloaddition appear to be greater than the transition-state energy

Table 4. Intramolecular Cycloadditions of Dienes Connected through All-Carbon-Containing Tethers to Cyclobutadiene

entry	substrate	cycloadducts	method[a]	yield (ratio)
(1)	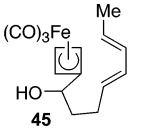	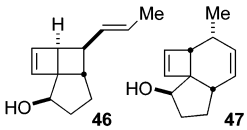	A	70% (1.0:1.8)
(2)	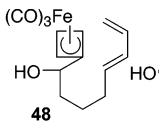	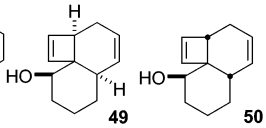	A	73% (2.4:1.0)
(3)	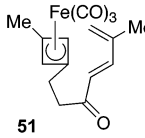	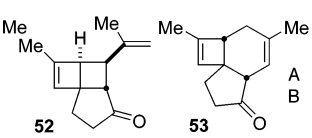	A B	0% 40%[c] (1:1)
(4)	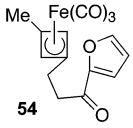	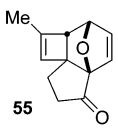	A B	0% 0%
(5)	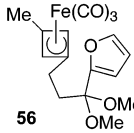	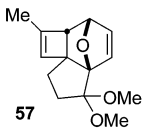	C	56%

[a] Reaction conditions. Method A: CAN (5 equiv), acetone (1 mM), RT, 10 min. Method B: TMAO (10 equiv), acetone (20 mM), reflux, 12 h. Method C: CAN (5 equiv), MeOH (1 mM), RT, 15 min. [b] Isolated yields. [c] Isolated as a mixture of cycloadducts **52**/**53** (1:1).

difference between the two modes of cycloaddition [i.e., (2 + 2) vs (4 + 2)]. In any event, as described earlier (e.g., Table 2), the (2 + 2) cycloadduct **46** can be converted readily via thermolysis to the corresponding (4 + 2) product **47** as a single diastereomer.

In contrast to substrates with a three-atom tether, the homologous four-atom tether complex **48** upon oxidation generates only the diastereomeric (4 + 2) cycloadducts **49** and **50** in 73% yield (**49**/**50**, 2.4:1; entry 2, Table 4). The fact that (2 + 2) cycloaddition is operative for three-atom diene tether substrate **45** and not for the corresponding four-atom tether **48** is consistent with previously described findings regarding (2 + 2) cycloadditions of three-atom carbocyclic olefin−tether complexes.[7c] That is, additional electronic activation of the four-atom tethered olefin is essential for an intramolecular cycloaddition to have a faster rate than competing cyclobutadiene dimerization.

We investigated next the feasibility of intramolecular cycloadditions involving three-atom all carbon-containing dienone complexes. When the disubstituted complex **51** was subjected to the typical CAN-promoted cycloaddition conditions, neither (2 + 2) nor (4 + 2) cycloadducts were obtained (entry 3, Table 4). On the other hand, when TMAO reaction conditions were employed, an equal mixture of cycloadducts **52** and **53** were obtained in 40% yield. Upon heating in pentanes (130 °C, 3 h), the mixture of these cycloadducts converged to the corresponding (4 + 2) cycloadduct **53**.

Treatment of the furan ketone complex **54** with either CAN or TMAO under typical reaction conditions did not afford any desired intramolecular cycloadducts. Cyclobutadiene dimers were obtained in the case with CAN, and with TMAO, a mixture of unidentifiable compounds and unreacted starting material (even after 20 equiv of TMAO) were obtained. While electronic activation of the olefin is expected to facilitate the cycloaddition, prior studies have shown that an sp^2 hybridized carbonyl group within the tether leads to sufficient bond angle strain in the (2 + 2) cycloaddition transition state to negate any electronic benefit.[7c] Evidently, the same trend may hold true for the (4 + 2) cycloaddition. In line with this possibility, the corresponding dimethyl ketal complex **56** undergoes an intramolecular (4 + 2) cycloaddition with CAN (MeOH, 1 mM, RT), to afford cycloadduct **57** in 56% yield (entry 5, Table 4).

Theoretical Calculations. Geometry optimizations were performed for all reactants, transition structures, and products using RB3LYP/6-31G(d) as implemented in Gaussian 98.[11] For diradical systems, optimizations were performed using UB3LYP/6-31G(d). All stationary points were characterized with frequency calculations. In general, two sets of energies are reported. The first energy value ($\Delta H^{\ddagger}$) is the relative enthalpy at 0 K, and the second energy value ($\Delta G^{\ddagger}$) is the relative free energy at 298 K.

Intermolecular Reactivity of Cyclobutadiene with Butadiene. Three transition structures are important for the characterization of the potential energy surface describing the reactivity of cyclobutadiene and butadiene. These transition structures are the (2 + 2) endo TS, the (4 + 2) endo TS, and the Cope rearrangement TS which interconverts the (2 + 2) and the (4 + 2) products. The remaining two transition structures, the (2 + 2) exo and (4 + 2) exo, are not directly relevant to understanding the intramolecular systems because, in general, exo products are not observed experimentally, but the exo transition structures are useful for comparisons of electronic character. The four cycloaddition transition structures will be abbreviated as (2 + 2)*n*, (4 + 2)*n*, (2 + 2)*x*, and (4 + 2)*x*.

The DA transition structure for cyclobutadiene plus ethylene is a synchronous (2 + 2) cycloaddition involving the delocalization of six electrons (Figure 2). What sets the cyclobutadiene system apart from typical DA transition structures (such as butadiene plus ethylene or cyclopentadiene plus ethylene) is the extremely low barrier ($\Delta H^{\ddagger} = 9.2$ kcal/mol) and the long C−C partial bonds (2.36 Å), indicating that the highly reactive cyclobutadiene combines with ethylene in a very early TS. The geometry of the cyclobutadiene moiety resembles the reactant, whereas butadiene and cyclopentadiene have TS geometries that are intermediate between those of reactant and product.

When the dienophile is changed from ethylene to butadiene, the (2 + 2)*n* TS undergoes an expected change from synchronous to asynchronous, such that the terminal partial C−C bond (A) is shorter than the internal partial C−C bond (B). In this case, what sets the cyclobutadiene apart is the minor change in the barrier of the DA reaction ($\Delta H^{\ddagger} = 9.1$ kcal/mol). For the

(11) Frisch, M. J.; Trucks, G. W.; Schlegel, H. B.; Scuseria, G. E.; Robb, M. A.; Cheeseman, J. R.; Zakrzewski, V. G.; Montgomery, J. A., Jr.; Stratmann, R. E.; Burant, J. C.; Dapprich, S.; Millam, J. M.; Daniels, A. D.; Kudin, K. N.; Strain, M. C.; Farkas, O.; Tomasi, J.; Barone, V.; Cossi, M.; Cammi, R.; Mennucci, B.; Pomelli, C.; Adamo, C.; Clifford, S.; Ochterski, J.; Petersson, G. A.; Ayala, P. Y.; Cui, Q.; Morokuma, K.; Malick, D. K.; Rabuck, A. D.; Raghavachari, K.; Foresman, J. B.; Cioslowski, J.; Ortiz, J. V.; Stefanov, B. B.; Liu, G.; Liashenko, A.; Piskorz, P.; Komaromi, I.; Gomperts, R.; Martin, R. L.; Fox, D. J.; Keith, T.; Al-Laham, M. A.; Peng, C. Y.; Nanayakkara, A.; Gonzalez, C.; Challacombe, M.; Gill, P. M. W.; Johnson, B. G.; Chen, W.; Wong, M. W.; Andres, J. L.; Head-Gordon, M.; Replogle, E. S.; Pople, J. A. *Gaussian 98*, revision A.9; Gaussian, Inc.: Pittsburgh, PA, 1998.

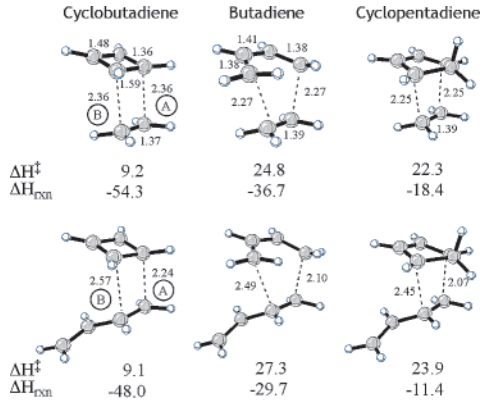

Figure 2. Effect of changing the dienophile from ethylene to butadiene on the activation enthalpy of Diels−Alder reactions of cyclobutadiene, butadiene, and cyclopentadiene.[12]

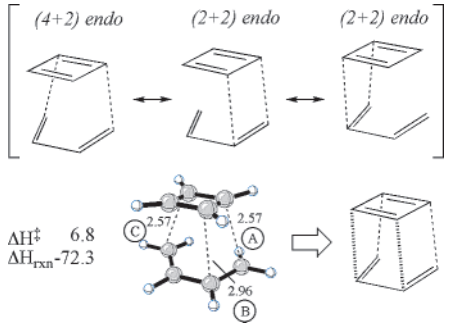

Figure 3. (4 + 2)*n* TS for the cycloaddition of cyclobutadiene and butadiene is stabilized by secondary orbital interactions.[12]

butadiene and cyclopentadiene systems, the DA barriers increase by ∼1.5−2.5 kcal/mol. In general, as reflected in Figure 2, butadiene is a less reactive dienophile than ethylene because π conjugation stabilizes the reactant more than the transition state. Similarly, reaction with butadiene leads to less favorable ΔH_{rxn} (by 6−7 kcal/mol) because the stabilizing π conjugation of the reactant is absent in the product. The (2 + 2)*n* TS with cyclobutadiene however, must be early enough that it is insensitive to the decrease in π conjugation of the butadiene dienophile.

Figure 3 shows the results for the (4 + 2)*n* cycloaddition of butadiene and cyclobutadiene. This mode of reaction is even more facile than the (2 + 2)*n* cycloaddition despite the energetic penalty of rotating the butadiene into the s-cis conformation. The TS is early and synchronous, with partial bonds A and C having lengths of 2.57 Å. It is noteworthy that the (4 + 2)*x* TS is much higher in energy than the (4 + 2)*n* TS, ($\Delta H^{\ddagger} = 9.1$ versus 6.8 kcal/mol), which suggests that the endo TS has additional favorable interactions that are absent in the exo TS. In the past, these "additional interactions" would have simply been attributed to secondary orbital overlap, but the recent work by Caramella and co-workers on bispericyclic transitions structures has elaborated on the special nature of the (4 + 2)*n* TS (Figure 4).[13] In Caramella's studies, the endo dimerization of cyclopentadiene proceeds through a C_2 symmetric TS that is simultaneously (4 + 2) and (2 + 4). In the optimized TS, the

(12) Energies are given in kcal/mol. Bond lengths are given in Å.

(13) (a) Caramella, P.; Quadrelli, P.; Toma, L. *J. Am. Chem. Soc.* **2002**, *124*, 1130. (b) Quadrelli, P.; Romano, S.; Toma, L.; Caramella, P. *Tetrahedron Lett.* **2002**, *43*, 8785. (c) Leach, A. G.; Houk, K. N. *Chemtracts* **2002**, *15*, 611. (d) Quadrelli, P.; Romano, S.; Toma, L.; Caramella, P. *J. Org. Chem.* **2003**, *68*, 6035.

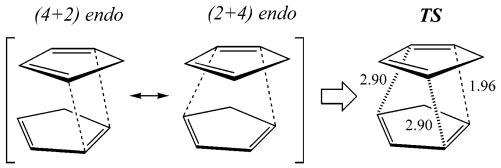

Figure 4. TS for dimerization of cyclopentadiene is bispericyclic. Two degenerate (4 + 2) cycloaddition paths contribute equally to the computed TS.

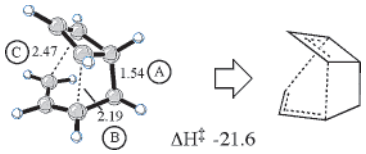

Figure 5. Cope rearrangement of the cyclobutadiene and butadiene endo cycloadducts. The Cope TS is +26.4 kcal/mol relative to the (2 + 2)*n* product and +50.7 kcal/mol relative to the (4 + 2)*n* product.

partial bond that is common to both the (4 + 2) and the (2 + 4) cycloadditions is extremely short (1.96 Å, Figure 4) while the other two partial bonds are very long (2.90 Å). The potential energy surface bifurcates after the cycloaddition, such that a single TS leads to both the (4 + 2) and the (2 + 4) products.[13]

In the case of cyclobutadiene plus butadiene, similar interactions are observed (Figure 3), but now three pericyclic processes are simultaneously present: the (4 + 2)*n*, the (2 + 2)*n*, and another (2 + 2)*n*. Partial bonds A and C are present in both the (4 + 2)*n* and the (2 + 2)*n* processes, but partial bonds B are only present in the (2 + 2)*n*. Consequently, in the optimized TS, bonds A and C are shorter than bonds B, and the cycloaddition leads only to the (4 + 2)*n* cycloadduct.

The formation of the (2 + 2)*n* product is less exothermic ($\Delta H_{rxn} = -48.0$ kcal/mol) than formation of the (4 + 2)*n* product ($\Delta H_{rxn} = -72.3$ kcal/mol) due to the cyclobutane ring strain in the former. These products can be interconverted by means of a boat Cope rearrangement. In the Cope TS, bond A is a fully formed σ bond, while bonds B and C are both partially formed (Figure 5). According to the Hammond postulate, the Cope TS should more closely resemble the less stable (2 + 2)*n* product, and indeed, it is observed that partial bond B is shorter than partial bond C.

Several predictions can be made from the above intermolecular model systems. First, because partial bond A is shorter in the (2 + 2)*n* cycloaddition with butadiene than with ethylene (Figure 2), the ideal tether length for an intramolecular (2 + 2)*n* of cyclobutadiene and butadiene will be shorter than the ideal tether length for the intramolecular (2 + 2) of cyclobutadiene and ethylene. Second, the ideal tether length for the (4 + 2)*n* intramolecular cycloaddition of cyclobutadiene and butadiene (Figure 3) will be significantly longer. Furthermore, because the (4 + 2)*n* TS has both (4 + 2) and (2 + 2) character, a short tether may skew this TS geometry to the point where it no longer leads to a (4 + 2)*n* product (formation of bonds A and C in Figure 3) but instead to the corresponding (2 + 2)*n* product (formation of bonds A and B in Figure 3). Finally, because bond A is fully formed in the Cope TS, this rearrangement should be relatively insensitive to the nature of the tether. These predictions are summarized in Figure 6.

Influence of the Tether on the Intramolecular Reactivity. Four model systems were chosen to study the intramolecular DA of cyclobutadiene tethered to butadiene. The four systems

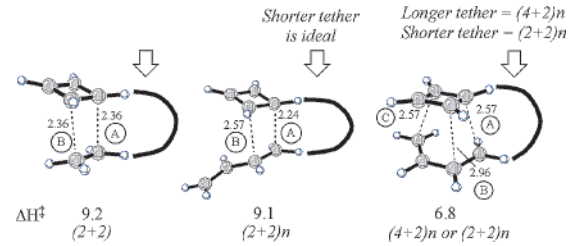

Figure 6. Intermolecular DA transition structures for cyclobutadiene and butadiene can be used to predict the influence of the tether on the intramolecular DA transition structures.

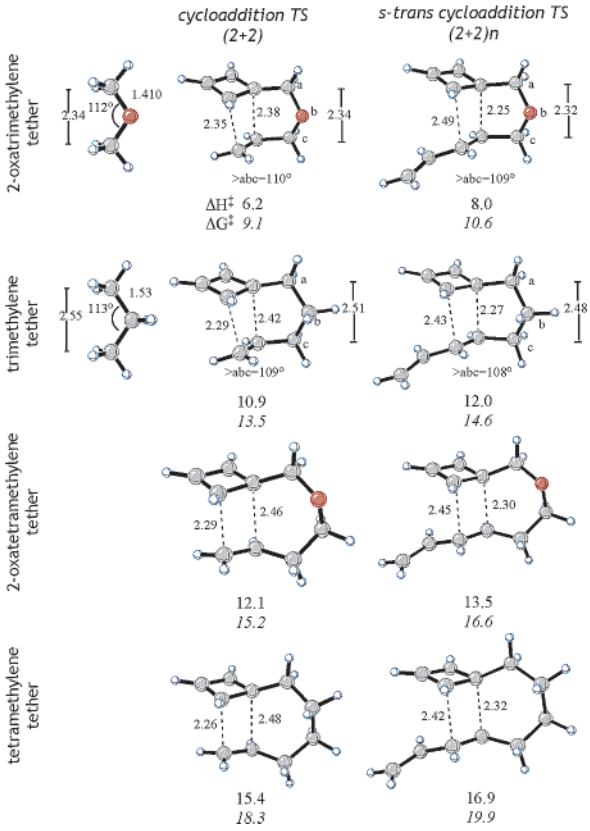

Figure 7. Transition structures for the intramolecular (2 + 2) reactions of cyclobutadiene with either a tethered ethylene or a tethered butadiene in the s-trans conformation. Tethers are shown on the left.[12]

differ only in the tether (2-oxatrimethylene, trimethylene, 2-oxatetramethylene, and tetramethylene) and correspond to the experimental reactions studied, involving **8**, **45**, **29**, and **48**, respectively. For each of these four model systems, the (2 + 2)*n*, (4 + 2)*n*, and Cope transition structures were calculated. Select exo transition structures were computed for comparison but were always higher in energy than the corresponding endo transition structures.

Figure 7 compares the geometries of the intramolecular (2 + 2) transition structures for cyclobutadiene plus ethylene[7c] with those for the intramolecular reactions of cyclobutadiene with s-trans butadiene. As predicted above, the intramolecular cycloadditions with butadiene do prefer shorter tethers than analogous cycloadditions with ethylene. For example, the ideal tether for the intramolecular DA of cyclobutadiene and ethylene is the 2-oxatrimethylene tether ($\Delta H^{\ddagger} = 6.2$ kcal/mol) because it allows excellent pericyclic orbital overlap between the cycloaddends without incurring any angle strain. When the same tether is used for the intramolecular DA reaction of cyclobutadiene and butadiene, the barrier of the reaction increases by 1.8 kcal/mol ($\Delta H^{\ddagger} = 8.0$ kcal/mol) because the ethereal tether must compress (leading to increased angle strain) to achieve favorable asynchronous bond formation where bond A is shorter than bond B. Similar effects are observed for four-atom tethers, but it is more difficult to illustrate the origin of the strain because there are changes in bond lengths, bond angles, and dihedral angles. In general, for a given tether, the barrier of the cycloaddition with ethylene is lower than the barrier with butadiene by 1.1−1.8 kcal/mol. Furthermore, as the natural tether length increases along the series, additional angle strain is necessary to achieve a good geometry for the cycloaddition. Taking the butadiene series as an example, the barrier increases from 8.0 kcal/mol to 12.0, 13.5, and 16.9 as the tether length increases.

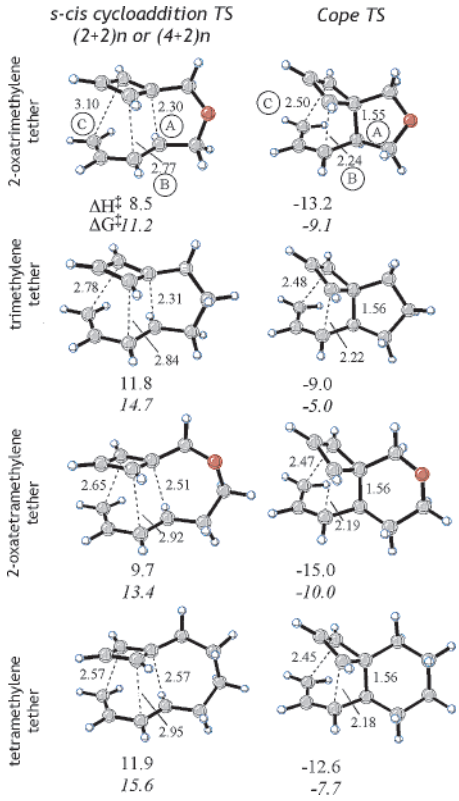

Figure 8. Transition structures for s-cis intramolecular cycloadditions between cyclobutadiene and butadiene and Cope rearrangements of the resulting cycloadducts. Four tethers of increasing length are examined: 2-oxatrimethylene, trimethylene, 2-oxatetramethylene, and tetramethylene. Energies are relative to the tethered cyclobutadiene reactant.[12]

When the butadiene adopts the s-cis conformation, the system can potentially undergo either an intramolecular (2 + 2)*n* or a (4 + 2)*n* cycloaddition. In general, only one distinct TS can be located and is often intermediate in character between the (2 + 2)*n* and the (4 + 2)*n* due to the geometric constraints of the tether. Consequently, all three partial bond lengths (A, B, and C) are important for characterizing these transition structures.

The cycloaddition transition structures involving s-cis diene conformations are shown in Figure 8. For the 2-oxatrimethylene tether, the cycloaddition corresponds to a (2 + 2)*n*, as suggested by the observation that partial bonds A and B are more fully formed than partial bond C. An intrinsic reaction coordinate (IRC) calculation confirms that the s-cis TS preferentially collapses to a (2 + 2)*n* and not to the (4 + 2)*n* product. In the absence of a tether, (4 + 2)*n* is preferred over (2 + 2)*n* by 2.3

Table 5. Summary of the Calculated Free Energies of Activation and Free Energies of Reaction for the Intramolecular Cycloaddition of Cyclobutadiene/Butadiene[12]

tether	s-trans TS: (2 + 2) $\Delta G^{\ddagger}$	s-cis TS: (2 + 2) or (4 + 2) $\Delta G^{\ddagger}$	Cope TS $\Delta G^{\ddagger}$	product (2 + 2) ΔG_{rxn}	product (4 + 2) ΔG_{rxn}	model for	exptl selectivity (2 + 2)/(4 + 2)
2-oxatrimethylene	10.6	11.2 (2 + 2)	−9.1	−38.6	−54.0	8 → 9 + 10	2.6:1.0
trimethylene	14.6	14.7 (4 + 2)	−5.0	−34.9	−51.1	45 → 46 + 47	1.0:1.8
2-oxatetramethylene	16.6	13.4 (4 + 2)	−10.0	−36.0	−59.1	29 → 30 + 31	1.0:13
tetramethylene	19.9	15.6 (4 + 2)	−7.7	−33.0	−57.6	48 → 49 + 50	0:100

kcal/mol, but the 2-oxatrimethylene tether is simply too short to allow the system to adopt the geometry necessary for the (4 + 2)*n* reaction. For the remaining three intramolecular systems, as the tether length increases, partial bond C becomes shorter and A becomes longer, such that the TS resembles the synchronous structure of the cyclobutadiene and butadiene (4 + 2)*n* TS; the s-cis TS now collapses to give the (4 + 2)*n* product. Additionally, as the tether increases in length, the energy difference between the barriers for the s-trans (2 + 2)*n* and the s-cis (4 + 2)*n* cycloadditions increases (Table 5).

The Cope transition structures are also shown in Figure 8. The tether length shows only a small effect on the geometry and relative energy of the Cope TS. A more noticeable effect is seen in the relative stabilities of the (2 + 2)*n* and (4 + 2)*n* products. For the three-atom tethers, the (4 + 2)*n* product is ∼15−16 kcal/mol more stable than the (2 + 2)*n* product. For the four-atom tethers, the (4 + 2)*n* product is ∼23−25 kcal/mol more stable than the (2 + 2)*n*.

Table 5 gives a summary of the computational results for the tethered cyclobutadiene and butadiene systems, and Figure 9 depicts the results in a generalized reaction coordinate. The calculated barriers for the (2 + 2)*n* and (4 + 2)*n* cycloaddtions are able to account for the experimentally observed selectivity in the reactions. For example, compound **8** gives predominantly the (2 + 2)*n* product, and the calculated cycloaddition transition structures both lead to the (2 + 2)*n* product. For **45**, the (2 + 2)*n* and (4 + 2)*n* products are both formed in substantial amounts, and the calculated barriers to form the products are essentially equal in height. For the 2-oxatetramethylene and the tetramethylene systems, the (4 + 2)*n* TS is significantly lower than the (2 + 2)*n*, and the experimentally observed ratios show high selectivity for the (4 + 2)*n* product.

Despite the success of theory in explaining the observed selectivity, this analysis is incomplete because two additional questions remain unanswered. (1) In our prior study of intramolecular cycloadditions of cyclobutadiene, the $\Delta G^{\ddagger}$ of the reaction needed to be less than ∼13.5 kcal/mol to compete successfully with cyclobutadiene dimerization (at a concentration of 10 mM). Now cycloadducts are observed in all of the above cases (experimental yields range from 70 to 75%) even though the lowest calculated barriers for the trimethylene and tetramethylene tethers are 14.6 and 15.6 kcal/mol, respectively. The high yields of these intramolecular cycloadditions can be attributed to the lower concentrations (1−2 mM) at which these reactions were run. This 10-fold dilution of the iron tricarbonyl complex and the oxidant may translate into a very slow formation of free cyclobutadiene; as a result, the concentration of free cyclobutadiene and therefore the intermolecular dimerization is reduced drastically at the higher dilutions. (2) Both (2 + 2)*n* and (4 + 2)*n* adducts are observed for the 2-oxatrimethylene tether even though calculations predict that both s-cis and s-trans cycloaddition transition structures lead exclusively to the (2 + 2)*n* product. Also, for the 2-oxatetramethylene tether, the s-trans TS is much higher in energy than the s-cis, yet both (2 + 2)*n* and (4 + 2)*n* products are observed. One possibility for the formation of the unexpected products is via the Cope rearrangement, but as highlighted in Scheme 1, no Cope interconversion of cycloadduct **9** is observed under kinetically controlled oxidative conditions. Two additional possibilities that have not yet been addressed are diradical mechanisms or a bifurcation of the potential energy surface after the s-cis TS, so that dynamic factors, in combination with the shape of the potential energy surface (PES), determine whether the s-cis conformation leads to the (2 + 2)*n* or the (4 + 2)*n* product.

A limited number of diradical mechanisms have been explored using UB3LYP/6-31G(d). The diradical addition of cyclobutadiene and butadiene is more favorable than the diradical addition of cyclobutadiene and ethylene. As shown in Figure 10, the first step of the mechanism is the rate-determining step and has a $\Delta H^{\ddagger}$ of 7.8 kcal/mol, which is 4.2 kcal/mol lower than the TS for diradical formation from cyclobutadiene and ethylene. Subsequent cyclization of the diradical intermediate

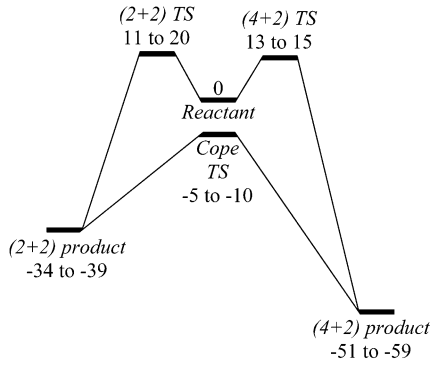

Figure 9. Conventional reaction coordinate for the intramolecular cycloaddition of tethered cyclobutadiene and butadiene. Free energies are taken from Table 5.[12]

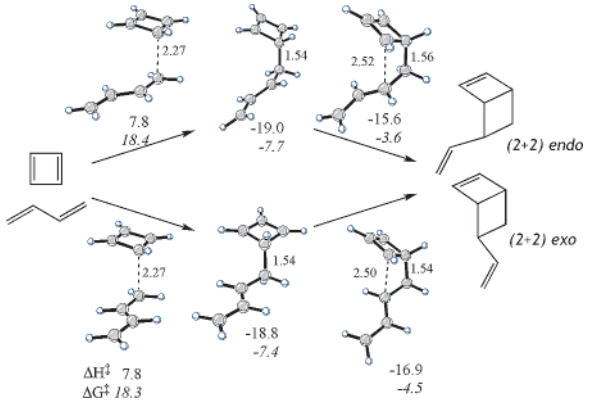

Figure 10. Stepwise diradical mechanisms of cyclobutadiene and butadiene to form (2 + 2)*n* and (2 + 2)*x* products.[12]

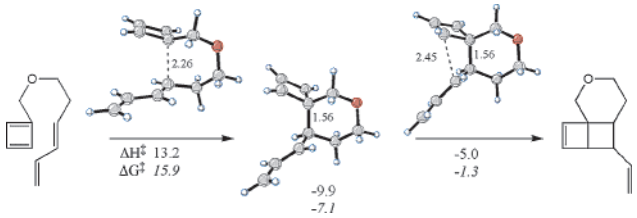

Figure 11. Stepwise diradical addition of the 2-oxatetramethylene system to form the (2 + 2)*n* product.[12]

leads to either the (2 + 2)*n* or the (2 + 2)*x* product. Thus far, we have been unsuccessful in locating a TS for the formation of the (4 + 2)*n* or (4 + 2)*x* products. Such transition structures are always difficult to locate because they involve rotational barriers in the diradical that bring radical centers into close proximity, such that they overlap to form the product without barrier.

Analogous diradical transition structures can be found for the intramolecular systems with four-atom tethers. An example is shown in Figure 11 for the 2-oxatetramethylene tether. Again the first step is the rate-limiting step. In this case, the barrier for the diradical addition ($\Delta H^{\ddagger} = 13.2$ kcal/mol) is higher than the barrier for concerted (4 + 2)*n* addition ($\Delta H^{\ddagger} = 9.7$ kcal/mol), and it appears that the diradical mechanisms should not be competitive with the pericyclic cycloadditions and are not operative for these systems.

Diradical pathways could not be computed for systems with three-atom tethers. For these systems, the diradical centers are constrained by the tether to be in close proximity. Consequently, the unrestricted (UB3LYP) wave functions collapsed to closed shell wave functions, and the calculations were optimized to the previously located concerted pericyclic transition structures.

Another explanation for the unexpected formation of both (4 + 2) and (2 + 2) products arises from specific features of the potential energy surface beyond the initial cycloaddition transition state. Reaction mechanisms are generally considered to be a linear series of transformations, such that one TS leads to the formation of a single product. Recent computational studies have shown, however, that this one-to-one relationship between TS and product is not true in all cases.[14] In the Caramella study of cyclopentadiene dimerization,[13] the bispericyclic TS leads to the formation of only one σ bond, and beyond this TS, the minimum energy path descends toward the Cope TS (Figure 12). Before reaching that stationary point, a valley ridge inflection breaks the C_2 symmetry, and then either the (4 + 2), or the (2 + 4) cyclopentadiene dimer can be formed with equal probability. The potential energy surface for the intramolecular reactivity of cyclobutadiene and s-cis butadiene is similar to that of cyclopentadiene dimerization, except the two pericyclic processes are not degenerate, and thus the (4 + 2) and the (2 + 2) products would not be expected to form in equal amounts.

Figure 13 shows a hypothetical contour plot representing the PES for the 2-oxatrimethylene system. On this graph, the *y*-axis corresponds to the formation of bond A, and the *x*-axis corresponds to the formation of either bond B or bond C. In the s-cis TS, bond B is more fully formed than bond C, which

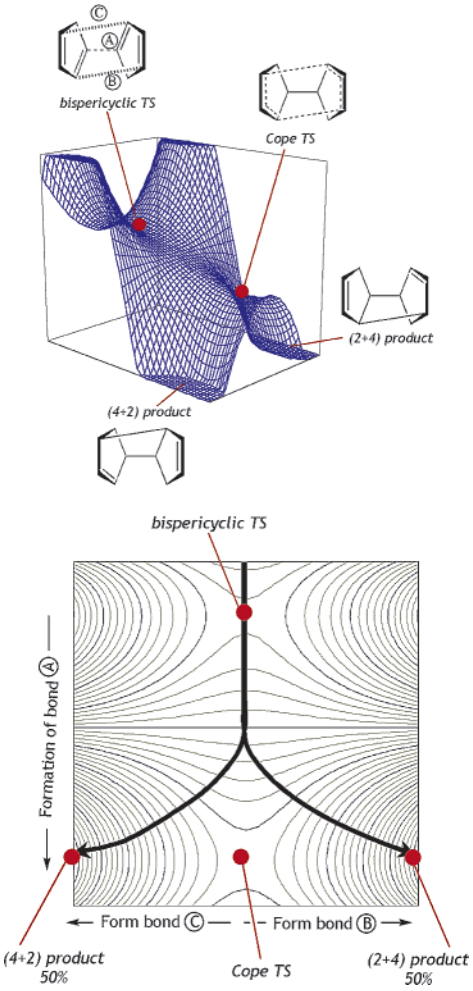

Figure 12. Potential energy surface and corresponding contour plot for cyclopentadiene dimerization. After the bispericyclic cycloaddition TS, a symmetric bifurcation in the energy surface results in the 50:50 formation of the (4 + 2) and (2 + 4) products.

is indicated by the TS placement to the right of center. In the Cope TS, bond A is now fully formed and bond B is still shorter than bond C, so again the TS is located to the right of center of the PES. A reactive trajectory for the system passes over the s-cis cycloaddition saddle point. Then, instead of continuing straight toward the Cope TS (which is a saddle point on the surface), a bifurcation takes place such that some trajectories lead to formation of the (4 + 2)*n* product and other trajectories lead to formation of the (2 + 2)*n* product. Because the s-cis cycloaddition TS and the Cope TS are approximately aligned on the *x*-axis, both the (4 + 2)*n* product and the (2 + 2)*n* product are formed in substantial amounts, even though the geometry of the cycloaddition TS suggests that only the (2 + 2)*n* product should be formed.

In contrast, the hypothetical PES for the tetramethylene system is shown in Figure 14. Here, the s-cis cycloaddition TS lies to the left of center because bond C is more fully formed than bond B. The Cope TS lies to the right of center because bond B is more fully formed than bond C. Because the s-cis TS and the Cope TS are staggered with respect to the origin of the x-axis, the s-cis TS is much more likely to form the (4 + 2)*n* product relative to the (2 + 2)*n* product.

Intermolecular Reactivity of Cyclic Dienes with Cyclobutadiene. Model systems of cyclobutadiene plus 1,2-dimeth-

(14) For a discussion of two-step, no-intermediate reactions, see: Singleton, D. A.; Hang, C.; Szymanski, M. J.; Meyer, M. P.; Leach, A. G.; Kuwata, K. T.; Chen, J. S.; Greer, A.; Foote, C. S.; Houk, K. N. *J. Am. Chem. Soc.* **2003**, *125*, 1319.

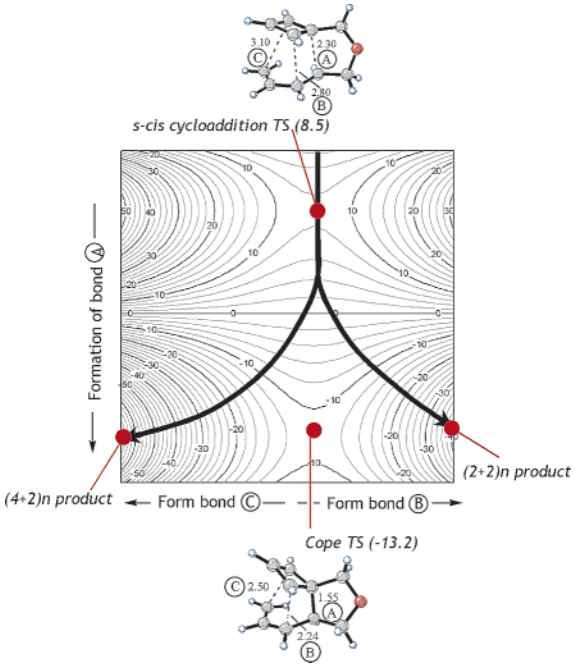

Figure 13. Hypothetical contour plot of the potential energy surface for the 2-oxatrimethylene tether, with butadiene in the s-cis conformation. The s-cis cycloaddition can lead to either the (4 + 2)*n* or the (2 + 2)*n* products because of a bifurcation on the surface. The shape of the PES (alignment of the s-cis TS and the Cope TS as well as the slopes of the surface) and the dynamic behavior of the system would determine the relative amounts of (2 + 2)*n* and (4 + 2)*n* product formed.

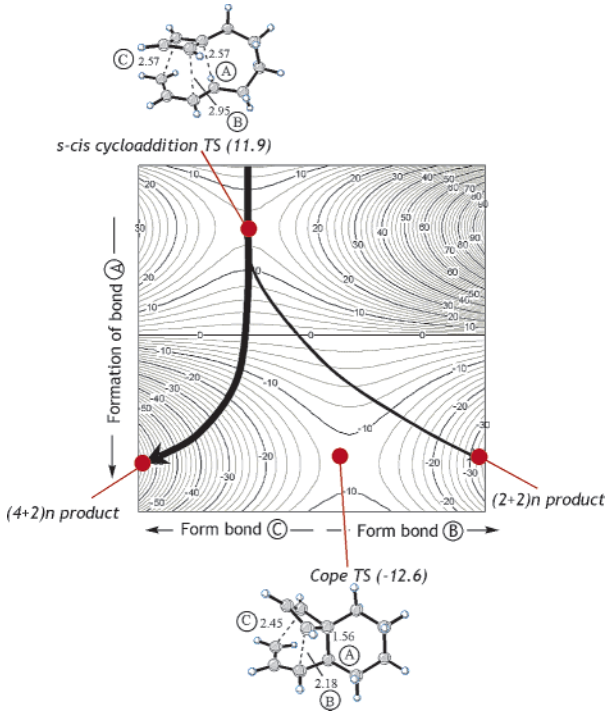

Figure 14. Hypothetical contour plot of the potential energy surface for the tetramethylene tether, with butadiene in the s-cis conformation. The s-cis cycloaddition would lead primarily to the (4 + 2)*n* product. The shape of the PES (alignment of the s-cis TS and the Cope TS as well as the slopes of the surface) and the dynamic behavior of the system would determine the relative amounts of (2 + 2)*n* and (4 + 2)*n* product formed.

ylenecyclopentane (DMCP), cyclopentadiene, and furan were studied to better understand the reactivity of various dienes with cyclobutadiene in the absence of a tether. Table 6 lists the energies of the (2 + 2) and (4 + 2) transition structures, as well as the partial bond lengths A, B, and C. DMCP, cyclopentadiene, and furan differ from butadiene in that they are locked into the s-cis conformation.

Table 6. Intermolecular Cycloadditions of Cyclobutadiene with 1,2-Dimethylenecyclopentane, Cyclopentadiene, and Furan[a]

Diene	(2+2)n TS			(2+2)x TS			(4+2)n TS		(4+2)x TS	
	$\Delta H^{\ddagger}$ kcal/mol	A (Å)	B (Å)	$\Delta H^{\ddagger}$ kcal/mol	A (Å)	B (Å)	$\Delta H^{\ddagger}$ kcal/mol	A/C (Å)	$\Delta H^{\ddagger}$ kcal/mol	A/C (Å)
	**9.1**	2.24	2.57	**9.1**	2.23	2.55	**6.8**	2.57	**11.2**	2.50
	-	-	-	**7.6**	2.24	2.66	**4.3**	2.54	**8.0**	2.48
	-	-	-	**9.9**	2.28	2.49	**4.2**	2.57	**9.5**	2.52
	-	-	-	**13.8**	2.13	2.48	**9.9**	2.38	**12.2**	2.38

[a] Activation enthalpies and partial bond lengths are given for the optimized transition structures. Butadiene is included for comparison.

The data in Table 6 point to several conclusions about the reactivity of cyclobutadiene with these s-cis dienes. The (2 + 2)*n* TS cannot be located for systems where the diene is locked into an s-cis conformation; instead, the system preferentially optimizes to the (4 + 2)*n* geometry. The (2 + 2)*x* transition structures are highly asynchronous, with partial bond A being 0.2−0.4 Å shorter than B. The (4 + 2) transition structures are synchronous. The (4 + 2)*n* is more stable than the (4 + 2)*x* because of secondary orbital interactions, originating in the dual (4 + 2)/(2 + 2) character of these transition structures. DMCP and cyclopentadiene are more reactive than butadiene because they are locked into s-cis conformation, whereas furan is less reactive than the other dienes because it is somewhat aromatic.

Intramolecular Reactivity of Cyclic Dienes with Cyclobutadiene. A second series of intramolecular cycloadditions and Cope transition structures was examined (Figure 15). For this series, the tether was constant (a 2-oxatrimethylene tether) and the diene was varied (butadiene, DMCP, cyclopentadiene, and furan). The previous discussion showed that the 2-oxatrimethylene tether is short, and in the case of butadiene, the inherent preference for (4 + 2)*n* reactivity can be disturbed by the short tether.

When the diene is locked in s-cis conformation, as in DMCP, the energy of the s-cis TS drops from 8.5 to 5.9 kcal/mol. The DMCP cycloaddition TS has bond lengths very similar to the butadiene s-cis TS, so it is not surprising that it also collapses to the (2 + 2)*n* product. The short ether tether is preventing significant overlap between the terminal end of the diene and cyclobutadiene, and consequently, partial bond B (2.8 Å) is more developed than C (3.1 Å).

Because cyclopentadiene is a reactive diene similar to DMCP but has a geometry similar to furan, it was included in this series even though experimental data are not available. Although cyclopentadiene is locked into s-cis conformation, it differs from DCMP in that the 1 and 4 carbons of the diene are forced to be much closer by the bridging methylene (Figure 15). As a result, the s-cis TS for cyclopentadiene is very low in energy, bond C is much shorter than was observed for the DMCP or butadiene transition structures, and it collapses to a (4 + 2)*n* product, as confirmed by an IRC calculation.

Table 7. Summary of the Calculated Free Energies of Activation and Free Energies of Reaction for the Intramolecular Cycloadditions of Cyclobutadiene with a 2-Oxatrimethylene Tether[12]

diene	s-trans TS: (2 + 2) $\Delta G^{\ddagger}$	s-cis TS: (2 + 2) or (4 + 2) $\Delta G^{\ddagger}$	Cope TS $\Delta G^{\ddagger}$	product (2 + 2) ΔG_{rxn}	product (4 + 2) ΔG_{rxn}	model for	exptl selectivity (2 + 2)/(4 + 2)
butadiene	10.6	11.2 (2 + 2)	−9.1	−38.6	−54.0	8 → 9 + 10	2.6:1.0
DMCP		9.6 (2 + 2)	−10.4	−37.6	−56.7	11 → 12 + 13	2.8:1.0
cyclopentadiene		8.2 (4 + 2)	−8.8	−38.1	−37.9		
furan		12.0 (4 + 2)	3.7	−25.9	−24.2	14 → 15 + 16	1.0:3.5

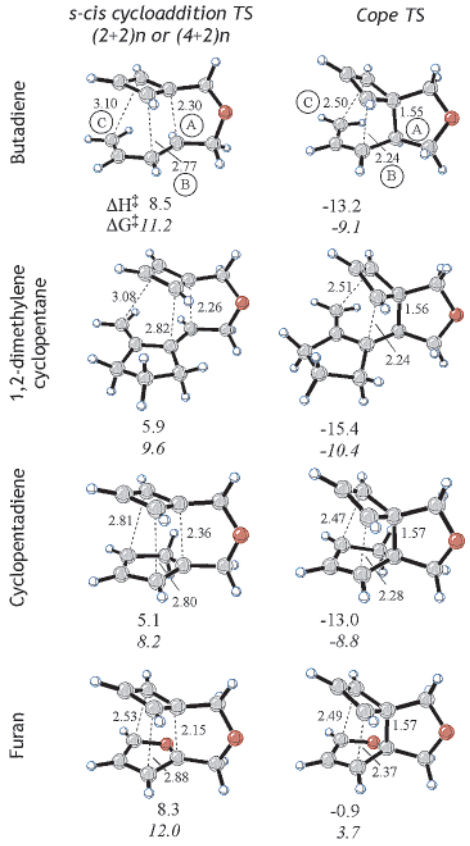

Figure 15. Transition structures for intramolecular cycloadditions between cyclobutadiene and various dienes (butadiene, 1,2-dimethylenecyclopentane, cyclopentadiene, and furan) and Cope transition structures of the resulting cycloadducts. A 2-oxatrimethylene tether is present in each system.[12]

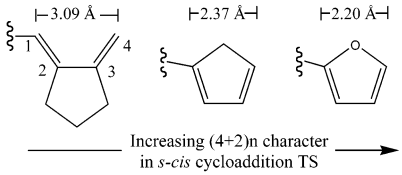

Figure 16. Calculated distances (B3LYP/6-31G*) of carbons 1 and 4 in the tethered s-cis dienes: 1,2-dimethylenecyclopentane, cyclopentadiene, and furan.

Furan differs from the other dienes because of its aromaticity. The s-cis TS is later and higher in energy than the cyclopentadiene TS because aromaticity stabilizes the ground-state reactant. As with cyclopentadiene, the compact geometry of furan allows for good overlap in a (4 + 2)*n* fashion, leading to short A and C bonds in the TS.

The trend for s-cis dienes is shown in Figure 16. As the C1−C4 distance of the diene becomes shorter, the s-cis cycloaddition TS has better (4 + 2) pericyclic overlap such that partial bond C is formed to a greater extent.

Table 7 shows a summary of the calculated free energies of activation and free energies of reaction for the intramolecular systems with the 2-oxatrimethylene tether. For this intramolecular series, the cycloaddition activation energies all fall below the 13.5 kcal/mol cutoff, and consequently, these substrates are expected to give minimal amounts of side products due to cyclobutadiene dimerization. It should also be noted that for the cyclopentadiene and furan systems, the (4 + 2)*n* is slightly less stable than the (2 + 2)*n* product; however, experimentally, the furan (2 + 2)*n* product can be converted to (4 + 2)*n* product under thermodynamic conditions.

The partial bond lengths B and C of the s-cis transition structures (Figure 15) are good predictors for whether the (2 + 2) product or the (4 + 2) product will be predominant. For example, in the DMCP system, the s-cis TS bond lengths are consistent with a (2 + 2)*n* cycloaddition, and the experimentally determined selectivity indicates that the (2 + 2)*n* product is the major product. Also, for the furan system, the s-cis TS is most consistent with a (4 + 2)*n* cycloaddition, and the observed major product is the (4 + 2)*n* product.

The formation of the minor cycloadduct can be understood in the context of a more detailed potential energy surface, such as those in Figures 13 and 14. The DMCP energy surface should resemble that in Figure 13 because both the s-cis TS and the Cope TS have (2 + 2)*n* character (i.e., partial bond B is shorter than C). This type of surface accounts for the formation of substantial amounts of (4 + 2)*n* product even though the s-cis cycloaddition TS appears to be a (2 + 2)*n* TS. On the other hand, the furan energy surface should more closely resemble that in Figure 14 because the s-cis TS has (4 + 2)*n* character (bond C is shorter than B) while the Cope TS has (2 + 2)*n* character (bond B is shorter than C). This type of surface accounts for the formation of a minor amount of (2 + 2)*n* product even though the s-cis TS appears to correspond to a (4 + 2)*n* cycloaddition. Using a similar analysis, we predict that the cyclopentadiene system would give less (2 + 2)/(4 + 2) selectivity than the furan system because the s-cis TS has less (4 + 2)*n* character than the analogous furan TS, but the (4 + 2)*n* product should still be the major product.

Conclusion

Oxidative decomposition of iron tricarbonyl complexes of substituted cyclobutadienes with CAN or TMAO liberates a free cyclobutadiene, which can be trapped intramolecularly with various dienes to afford highly functionalized cyclobutene-containing cycloadducts. Generally, substrates that fail to undergo the intramolecular cycloadditions under the fast CAN-promoted reaction conditions cyclize to afford the corresponding cycloadducts when the slower oxidant, TMAO, is employed.

When dienes are used as the cycloaddition partner for cyclobutadiene, depending on the nature of the tethers, both (2

+ 2) endo and (4 + 2) endo adducts or just (4 + 2) endo cycloadducts are obtained in moderate-to-good yields. In general, most carbocyclic and long ether−tether complexes (i.e., four-atom tether or longer) favor the intramolecular (4 + 2) cycloadditions, where the cyclobutadiene functions as a dienophile. Furthermore, any (2 + 2) cycloadduct obtained during the reaction can be isomerized thermally to the corresponding identical endo (4 + 2) cycloadduct via a [3,3]-sigmatropic rearrangement.

Computational results reveal that a number of factors influence the (2 + 2)/(4 + 2) selectivity of the intramolecular cycloadditions of cyclobutadiene with dienes. In the absence of a tether, cyclobutadiene prefers to react with a diene in a (4 + 2)*n* cycloaddition because of stabilizing secondary orbital interactions. The presence of a tether constrains the geometry of the system and, hence, the pericyclic overlap of the cycloaddition, which is the reason shorter tethers favor the (2 + 2)*n* cycloaddition while longer tethers favor the (4 + 2)*n* cycloaddition.

The tethered dienes can be divided into two broad classes: those that can adopt either the s-trans or the s-cis conformation and those that are locked into s-cis conformation. Butadiene is the model for the former category; these systems can undergo two distinct intramolecular cycloadditions (with the butadiene in the s-trans conformation or in the s-cis conformation), whereas for dienes locked in s-cis conformation, only one cycloaddition TS is possible. The s-cis cycloaddition can lead potentially to either the (4 + 2) or the (2 + 2) product due to a bifurcation in the potential energy surface after the TS. A diene with a shorter C1−C4 distance has better (4 + 2) overlap and leads to higher (4 + 2) selectivities, and a diene with a longer C1−C4 distance (the extreme case being butadiene in s-trans conformation) has poorer (4 + 2) overlap and leads to higher (2 + 2) selectivities.

Overall, the highly functionalized cyclobutene-containing cycloadducts obtained in this intramolecular cycloaddition offer new opportunities for efficient construction of complex synthetic targets. In this regard, studies to exploit the potential of these novel intermediates are currently in progress.

Experimental Section

General Methods. All reactions were carried out under N_2 atmosphere in oven-dried glassware (120 °C, 12 h) using standard air-free manipulation techniques.

All reaction solvents were purchased from commercial sources and purified as follows: pentanes and CH_2Cl_2 were distilled over CaH_2 under N_2; THF, Et_2O, and benzene were distilled over Na/K and benzophenone under N_2 immediately prior to use. HPLC-grade acetone and MeOH were used in the cycloaddition without further purification and kept under N_2 atmosphere. Chromatographic solvents, such as hexanes, pentanes, and Et_2O were purified by simple distillation. All other commercially available reagents were purified by either simple distillation or recrystallization.

Concentration in vacuo refers to removal of solvent(s) using a Büchi rotary evaporator at 40−80 Torr followed by the use of vacuum pump at approximately 1 Torr. The use of brine refers to saturated aqueous (aq) NaCl. Silica gel flash column chromatography was performed using EM Science Silica Gel 60 Geduran (35−75 μm). Alumina gel flash chromatography was carried out using either Aldrich or Macherey-Nagel 58 Å neutral, activated Brockmann type I Al_2O_3 (~150 mesh). Analytical thin-layer chromatography (TLC) was performed with 0.25-mm EM silica gel $60F_{254}$ plates. Gas chromatography (GC) analyses were carried out using HP 5890 Series II spectrometer with a 30-m HP1 capillary fused column.

Proton (^{1}H) nuclear magnetic resonance (NMR) spectra were measured on Varian Gemini-300 (300 MHz), Gemini-400 (400 MHz), or Gemini-500 (500 MHz) instrument. Carbon (^{13}C) nuclear magnetic resonance (NMR) spectra were recorded using either Varian Gemini-75 (75 MHz), Gemini-100 (100 MHz), or Gemini-500 (125 MHz) instrument with complete proton decoupling mode. Chemical shifts are reported in ppm downfield from tetramethylsilane. Infrared (IR) spectra are reported in wavenumbers and measured on either a Nicolet 510 FT-IR or Perkin-Elmer 1310 instrument. Gas chromatography−mass spectroscopy (GC−MS) spectra were recorded using an HP 5890 Series II GC instrument coupled to an HP 5972 Mass Selective Detector. Melting points are reported without correction or calibration. Elemental analyses were performed by the analytical laboratory of Robertson Microlit Laboratories, Inc., Madison, NJ 07940.

Cycloaddition Methods. Unless otherwise noted, all of the oxygen- and enone-containing tricarbonylcyclobutadiene−iron complex substrates were prepared according to the published procedures.[15] The intramolecular cycloadditions were promoted by oxidative removal of the iron from its corresponding cyclobutadiene ligand according to one of the following methods:

Method A. CAN-promoted cycloadditions: To a solution of the tricarbonylcyclobutadiene iron complex (1.0 equiv) under N_2 atm in either HPLC-grade acetone or MeOH (1−3 mM) was added CAN (5.0 equiv) as a solid over 3 min at RT. The resulting orange solution was stirred for 10 min, then neutralized with saturated $NaHCO_3$ solution and transferred to a separatory funnel containing Et_2O and H_2O. The aqueous layer was separated and back-extracted with Et_2O (2×). The combined organic layer was washed with H_2O and brine, dried over $MgSO_4/K_2CO_3$, filtered and concentrated in vacuo, and purified by silica gel flash column chromatography.

Method B. TMAO-promoted cycloadditions: To a solution of the tricarbonylcyclobutadiene iron complex (1.0 equiv) under N_2 atm in HPLC-grade acetone (1−40 mM) was added a portion of TMAO (4−10 equiv). The resulting reaction mixture was refluxed for 6 h, treated with a second portion of TMAO (4−10 equiv), and refluxed for additional 6−18 h. Once all starting material had been consumed as judged by TLC and GC, the resulting brown suspension was cooled to RT and then transferred to a separatory funnel containing Et_2O and saturated $NaHCO_3$ solution. The aqueous layer was separated and back-extracted with Et_2O. The combined organic layer was washed with H_2O and brine, dried over $MgSO_4/K_2CO_3$, filtered, concentrated in vacuo, and purified by silica gel flash column chromatography.

Thermal Rearrangements. In the case of cycloadditions, where two possible modes of closure are operative, thermal isomerization of any (2 + 2) product formed during the cycloadditions to the corresponding (4 + 2) cycloadduct was carried out by heating the (2 + 2) substrate in pentanes to 130 °C for 2.5 h in a sealed tube under N_2 atmosphere. The reaction mixtures were allowed to cool to RT, and the solvent was removed under reduced pressure at 0 °C. The resulting residues were purified by silica gel flash column chromatography.

Acknowledgment. M.L.S. thanks the National Institute of General Medical Sciences (National Institutes of Health, GM62824) for financial support. K.N.H. thanks the National Science Foundation (CHE-9986344) for financial support. K.S.K. thanks the National Science Foundation for a Graduate Fellowship.

Supporting Information Available: Experimental procedures, data on new compounds, and computational results are provided (PDF). This material is available free of charge via the Internet at http://pubs.acs.org.

JA0380547

(15) See ref 7 and Porter, J. R.; Snapper, M. L. *Synthesis* **1999**, 1407.